doi: 10.15407/ujpe62.04.0335

V.I. BOICHUK, I.V. BILYNSKYI, R.I. PAZYUK

Department of Theoretical and Applied Physics and Computer Simulation,
Ivan Franko State Pedagogical University of Drohobych
(3, Stryiska Str., Drohobych 82100, Ukraine; e-mail: ri.pazyuk@gmail.com)

MINIBAND ELECTRICAL CONDUCTIVITY IN SUPERLATTICES OF SPHERICAL InAs/GaAs QUANTUM DOTS

PACS 73.21.Cd, 68.65.Cd

The electrical properties of nanoscale semiconductor InAs/GaAs heterosystems with 2D-superlattices of spherical quantum dots have been studied. The dependences of the electron group velocity on the wave vector and the miniband quantum number are obtained. The dependences of the Fermi level of electrons in minibands on the concentration of donor impurities, donor energy, and temperature are found. The temperature dependences of the majority carrier concentration and the electrical conductivity are analyzed for various donor concentrations and energies.

K e y w o r d s: quantum dot, superlattice, electron states, miniband, electrical conductivity.

1. Introduction

Creation of synthetic materials with prescribed physical properties that cannot be found in the Nature is one of the major tasks of modern science and engineering. Modern nanomaterial technologies are capable of creating systems composed of hundreds and even thousands of nanodimensional building blocks with extremely diverse structures. One of the most promising types of those blocks includes semiconductor quantum dots (nanocrystals), which are often called "artificial atoms" because of their discrete energy spectrum for various quasiparticles, e.g., electrons (holes) and excitons [1–3].

A significant interest in nanocrystals (NCs) during the last decades is explained by their unique physical properties [4–7] and the capability to modify the latter by varying the nanocrystal volume. Interaction of NCs with one another and with external electromagnetic fields depends on the NC dimensions and geometry, as well as on the presence of impurities in them [8–13]. Those dependences are applied in various electronic and optoelectronic devices, including NC-based lasers [14–16], single-photon sources [17–19], solar cells [20–22], and photodetectors [23–25].

In the last decade, considerable attention of researchers was focused on multibarrier and superlattice nanoheterostructures. In works [26–28], the models of effective electron masses and rectangular potentials were used to develop the theory of dynamic electron conductivity in multibarrier structures with either a plane or cylindrical shape.

Work [29] was devoted to the study of superlattices of tunnel-coupled GaAs nanocrystals periodically located in the $Al_xGa_{1-x}As$ matrix along an elliptic quantum wire. It was shown that the energy spectrum of electrons in such superlattices consists of a number of energy minibands, the positions and the number of which are determined by the NC size. The widths of the allowed and forbidden minibands depend on the thicknesses and heights of potential barriers.

The authors of works [30, 31] presented models of three-dimensional superlattices, cubic and tetragonal, for InAs nanocrystals/GaAs and Ge/Si heterosys-

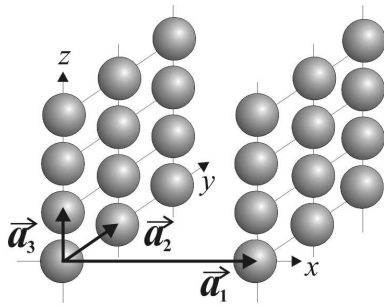

Fig. 1. Geometrical diagram of a two-dimensional superlattice of spherical nanocrystals

tems. The electron and phonon spectra of those superlattices were calculated. The dependences of the effective electron mass tensor and the electron conductivity on the main superlattice parameters were analyzed. The superlattice properties were found to be more sensitive to the dot-to-dot distance than to the NC shape.

The energy spectrum and optical properties of superlattices consisting of spherical nanocrystals were studied in works [32, 33]. The electron energy distributions in the $1s$- and three $1p$-subbands were calculated for various NC radii and Al concentrations in the $Al_xGa_{1-x}As$ matrix. The coefficients of intersubband light absorption were determined for various polarizations of light incident on the array of one-dimensional ordered chains of spherical NCs.

This research is a logical continuation of the cited works. A model of two-dimensional superlattice systems InAs/GaAs is considered. The dependences of the electrical conductivity on the Fermi quasilevel position and the donor concentration in the matrix are analyzed.

2. Statement of the Problem

As a superlattice, we consider the system, in which the unit cell is a rectangular prism with the edge lengths a_1, a_2, and a_3 (Fig. 1). If the distance between the centers of nanocrystals, e.g., along the OX axis (a_1) is so large that the NCs can be regarded as noninteracting, the system is called a two-dimensional superlattice of spherical nanocrystals.

Let us consider InAs nanocrystals in the GaAs matrix, when the neighbor NCs located in the same plane, e.g. OYZ, are considered to interact with each other. In order to calculate the energy spectrum of an electron in this heterostructure, we will use the step-potential approximation. In addition, we will assume that the effective electron mass changes its value at the interface, in a very narrow region of coordinates. Therefore, the potential energy and the electron mass look like

$$\begin{aligned} V(r) &= \begin{cases} -U_0, & r \le R, \\ 0, & r > R, \end{cases} \\ m(r) &= \begin{cases} m_1, & r \le R, \\ m_2, & r > R, \end{cases} \quad U_0 > 0, \end{aligned} \tag{1}$$

respectively, where r is the distance of the electron from the NC center, and $U_0 > 0$.

The Schrödinger equation for a spherical NC provided conditions (1) has exact solution. The wave functions of the electron states were obtained in the form [32]

$$\phi_\nu(\mathbf{r}) = \left\{ \begin{matrix} A\, j_l(kr), & r \le R \\ B\, h_l^{(1)}(\chi r), & r > R \end{matrix} \right\} Y_{l\,m}(\theta, \phi),$$

where $k = \sqrt{\frac{2m_1(U_0+E^0)}{\hbar^2}}$, $\chi = \sqrt{\frac{2m_2E^0}{\hbar^2}}$, $E^0 < 0$, $Y_{l\,m}(\theta, \varphi)$ is the spherical function, and $j_l(x)$ and $h_l^{(1)}(x)$ are the Bessel and Hankel functions, respectively. From the matching conditions for the wave function, which involve the continual character of the wave function itself and the probability flow, it is possible to determine the energy E_ν^0 of electron quantum states in the NC:

$$\begin{vmatrix} j_l(kR) & -h_l^{(1)}(\chi R) \\ \dfrac{1}{m_1} j_l'(kR) & -\dfrac{1}{m_2} h_l^{(1)\prime}(\chi R) \end{vmatrix} = 0. \tag{2}$$

In order to find the energy spectrum and the wave functions of an electron in the two-dimensional superlattice of spherical nanocrystals, it is necessary to solve the Schrödinger equation with the Hamiltonian [32]

$$\mathbf{H} = -\frac{\hbar^2}{2} \nabla \frac{1}{m(\mathbf{r})} \nabla + U(\mathbf{r}),$$

where $U(\mathbf{r})$ is the periodic superlattice potential. Since the main parameters of the crystals in the heterostructure (the lattice constants and the dielectric permittivities) are close to each other, let us choose the potential $U(\mathbf{r})$ as the sum of potentials created by nanocrystals,

$$U(\mathbf{r}) = \sum_{\mathbf{n}} V(\mathbf{r} - \mathbf{n}),$$

where $\mathbf{n} = n_1 a_1 + n_2 a_2 + n_3 a_3$ ($n_i = 0, \pm 1, \pm 2, \pm 3, ...$).

The wave function of an electron in the superlattice, $\psi(\mathbf{r})$, has to satisfy the condition $\psi(\mathbf{r}+\mathbf{n}) = e^{i\mathbf{kn}}\psi(\mathbf{r})$. We are interested in the subbarrier energy bands of the superlattice, i.e. the subbands with the energy lower than the barrier height at the nanocrystal-matrix interface. Let us consider NCs with dimensions and distances between them such that the overlap integrals for the wave functions of neighbor NCs are small. In this case, the widths of the subbands of various types are much smaller than the distances between the subbands. Provided those conditions, the strong coupling approximation allows one to obtain not only qualitatively, but also quantitatively correct results when calculating the electron dispersion laws [34]. The wave function of the electron in the superlattice, $\psi(\mathbf{r})$, is tried in the form

$$\psi(\mathbf{r}) = \sum_{\mathrm{n},\nu} C_\nu e^{i\mathbf{kn}} \phi_\nu(\mathbf{r}-\mathbf{n}), \tag{3}$$

where $\phi_\nu(\mathbf{r})$ are the eigenfunctions of the energy operator for the electron in the NC.

In the nearest-neighbor approximation, the following dispersion equation is obtained for the energy of superlattice electrons:

$$\sum_\nu C_\nu \left[\left(E^0_{\nu'} - E(\mathbf{k})\right) \left(\delta_{\nu\nu'} + 2\sum_{i=1}^{3} A^i_{\nu\nu'} \cos(k_i a_i)\right) + 2\sum_{i=1}^{3} \left(B^i_{\nu\nu'} + P^i_{\nu\nu'} \cos(k_i a_i)\right)\right] = 0. \tag{4}$$

Here, the following notations are introduced for convenience:

$$\begin{aligned} A^i_{\nu\nu'} &= \int \phi^*_{\nu'}(\mathbf{r}-\boldsymbol{a}_i)\,\phi_\nu(\mathbf{r})\,d\mathbf{r}, \\ B^i_{\nu\nu'} &= \int \phi^*_{\nu'}(\mathbf{r})\,V(|\mathbf{r}-\boldsymbol{a}_i|)\,\phi_\nu(\mathbf{r})\,d\mathbf{r}, \\ P^i_{\nu\nu'} &= \int \phi^*_{\nu'}(\mathbf{r}-\boldsymbol{a}_i)\,V(|\mathbf{r}-\boldsymbol{a}_i|)\,\phi_\nu(\mathbf{r})\,d\mathbf{r}. \end{aligned} \tag{5}$$

The superlattice electron subbands with the dispersion law $E = E(\mathbf{k})$ can be filled, after the heterosystem is doped with donor impurities. This doping makes it possible to obtain the electron subsystem in the thermodynamic equilibrium state. In order to create a directed flux of charge carriers, one should violate the symmetry of the distribution function [34], i.e. disturb the system of charges from the equilibrium state. It can be reached by embedding the heterosystem into an external electric field. If the strength of this field is relatively low, the vector of current density is determined by the following general formula:

$$\mathbf{j} = \frac{e^2\tau(T)}{4\pi^3}\int \mathbf{v}\frac{\partial f}{\partial E}(\mathbf{v}, \nabla_r\Phi)\,d\mathbf{k}, \tag{6}$$

where f is the electron distribution function, v the average electron velocity, and $\tau(T)$ the relaxation time. The strength of the external electrostatic field is expressed in terms of the scalar potential Φ as $\mathbf{E} = -\nabla_r\Phi$.

When calculating the tensor of conductivity for the superlattice with nanocrystals, the contributions of all filled electron minibands in the structure have to be taken into consideration,

$$\sigma_{\alpha\beta} = \sum_n \sigma^{(n)}_{\alpha\beta},\ \alpha,\beta = 1,2,3. \tag{7}$$

The components of the tensor of conductivity of the heterosystem look like

$$\sigma^{(n)}_{\alpha\beta} = \frac{e^2\tau(T)}{4\pi^3 k_\mathrm{B}T}\iiint\limits_{BZ} v^{(n)}_\alpha(k_1,k_2,k_3)\,v^{(n)}_\beta(k_1,k_2,k_3)\times \times \frac{\exp\left[\frac{E^{(n)}(k_1,k_2,k_3)-E_\mathrm{F}}{k_\mathrm{B}T}\right]}{\left\{\exp\left[\frac{E^{(n)}(k_1,k_2,k_3)-E_\mathrm{F}}{k_\mathrm{B}T}\right]+1\right\}^2} dk_1dk_2dk_3. \tag{8}$$

Here, the following notations are used: e is the elementary charge, k_B the Boltzmann constant, T the temperature, E_F the Fermi level in the electron subsystem, $v^{(n)}_j(k_1,k_2,k_3)$ the j-th component of the group velocity vector of the electron in the n-th subband, and $\mathbf{k}(k_1,k_2,k_3)$ the electron wave vector. The integration in Eq. (8) is carried out over the quasi-Brillouin zone.

The Fermi level position is determined from the condition of electroneutrality, i.e. provided that the number of electrons in the electron subbands is equal to the number of holes on the donor levels. Let us consider the case of doping with monovalent impurity atoms of the same kind. Then we obtain the following equation for the Fermi energy as a function of the temperature:

$$\sum_{n,\mathbf{k}} \frac{2}{\exp\left(\frac{E^n(\mathbf{k})-E_\mathrm{F}}{k_\mathrm{B}T}\right)+1} = \frac{n_\mathrm{D}}{\exp\left(\frac{E_\mathrm{F}-E_\mathrm{D}}{k_\mathrm{B}T}\right)+1} + \sum_{\mathbf{k}} \frac{2n_\mathrm{D}}{\exp\left(\frac{E_\mathrm{F}+E_G+\frac{\hbar^2k^2}{2m_h}}{k_\mathrm{B}T}\right)+1}, \tag{9}$$

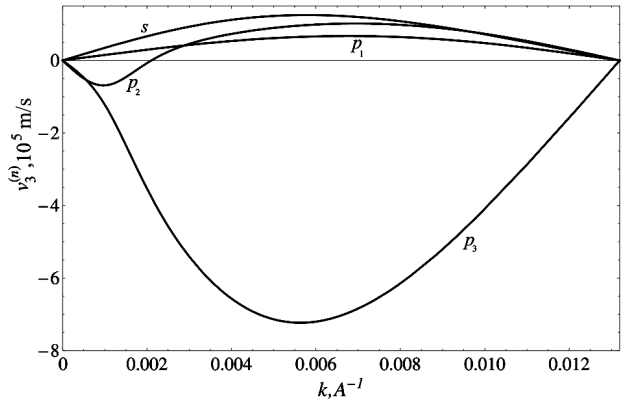

Fig. 2. Group velocities of electrons in the s-, p_1-, p_2-, and p_3-subbands in the 2D superlattice InAs/GaAs with spherical NCs of the radius $R = 60$ Å

where n_{D} is the donor concentration, E_{D} the donor level energy, E_G the forbidden gap width, and m_h the hole effective mass.

Formula (8) demonstrates that the conductivity $\sigma_{\alpha\beta}^{(n)}$ is also governed by the relaxation time $\tau(T)$. For simplicity, the majority of authors assume that the relaxation time τ_0 is constant [30] and equal, for example, to $\tau_0 = 10^{-12}$ s. If the temperature changes a little, this assumption is justified in the first approximation. However, the results of researches concerning the intersublevel relaxation time of electrons in the InAs/GaAs superlattices [35] testify to its considerable nonlinear variation with the temperature. This dependence, $\tau = \tau\,(T)$, arises owing to the electron scattering by both phonons and donor centers. In particular, $\tau_0 = 35$ ps for the room temperature $T = 300$ K, whereas $\tau_0 = 347$ ps for $T = 15$ K. The maximum variation rate is observed in the temperature interval from 120 to 200 K. Therefore, the further calculations in this work will be carried out, by taking the dependence $\tau = \tau\,(T)$ into account.

From formula (8), one can also see that the conductivity tensor depends on the dispersion of electrons and their group velocity. The group velocity of electrons is determined by the number of the structure miniband and the corresponding dispersion law $E^n\,(\mathbf{k})$,

$$v_{\alpha}^{(n)}\,(k_1, k_2, k_3) = \frac{1}{\hbar}\frac{\partial E^{(n)}\,(k_1, k_2, k_3)}{\partial k_{\alpha}}. \qquad (10)$$

As a example, let us calculate the electron velocities in the s-, p_1-, p_2-, and p_3-like subbands as functions of the k_3 component of the electron wave vector, provided that the other projections of the wave vector $\mathbf{k}$ equal zero for the 2D superlattice.

3. Analysis of the Results Obtained

Specific numerical calculations were performed for superlattices of the InAs/GaAs heterosystem with the following parameters: $m_{1\,e} = 0.023m_0$, $m_{2\,e} = 0.0665m_0$, and $V_e = 0.775$ eV. For simplicity, we adopt that, for the 2D superlattice, $a_2 = a_3 \equiv a \ll a_1$, $a = 2R + d$, and $d = 6$ Å.

In Fig. 2, the dependences of the electron group velocities in various subbands of the InAs/GaAs superlattice on the electron wave vector magnitude $|k_3| \leq \pi/a$ are shown for the case of NCs with the radius $R = 60$ Å. One can see that, for the fixed wave vector, the electron group velocity strongly depends on the miniband index, because the functions $E^{(n)} = E^{(n)}(\mathbf{k})$ have different behaviors for positive wave-vector projections.

The calculation results obtained for the function $E_{\mathrm{F}} = E_{\mathrm{F}}\,(T)$ at various donor concentrations n_{D} and E_{D} are exhibited in Fig. 3. In Fig. 3, *a,* the temperature dependences of the Fermi level are shown for the impurity concentration $n_{\mathrm{D}} = 4.64 \times 10^{10}$ cm^{-2} and various donor level energies E_{D}. The energy E_{D} is reckoned from the bottom of the conduction band in the GaAs matrix. One can see that, for E_{D} varying from -850 to -300 meV (curves *1* to *6*), the dependences $E_{\mathrm{F}} = E_{\mathrm{F}}\,(T)$ reveal a characteristic minimum. The calculations showed that, at $E_{\mathrm{D}} > -550$ meV (curves *4* to *6* in Fig. 3, *a*), the change of the ionization energy E_{D} practically does not affect the behavior of the function $E_{\mathrm{F}}\,(T)$. At the same time, for $E_{\mathrm{D}} < -550$ meV (curves *1* to *3*), a substantial difference between the Fermi level positions is observed at the temperatures $T < 200$ K, unlike room ones.

Changes in the donor impurity concentration n_{D} in the GaAs matrix (Fig. 3, *b*) make the dependence $E_{\mathrm{F}}\,(T)$ more pronounced. As the donor concentration n_{D} diminishes, the minimum in the energy dependence $E_{\mathrm{F}}\,(T)$ increases by absolute value and shifts toward low temperatures (curves *1–3* and *4–6* in Fig. 3, *b*). In this region, the dependence $E_{\mathrm{F}}\,(T)$ is mainly governed by the energy of donor level ionization, E_{D}. However, at low n_{D}, as the temperature grows, the Fermi energy becomes independent of the

donor energy $E_{\rm D}$ already at $T > 150$ K (curves *1* and *4*). This behavior of the Fermi level energy affects the temperature dependence of the carrier concentration and, as a consequence, the conductivity of this system.

Let the vector of the electric field strength be directed along the coordinate axis OZ, i.e. in parallel to the vector $\boldsymbol{a}_3$ (Fig. 1). In this case, the specific conductance σ for the examined superlattice equals σ_{33}. The corresponding calculations showed that, depending on the donor level energy, two scenarios are possible for the temperature dependences of the charge carrier concentration n (Fig. 4) and the specific conductance σ (Fig. 5). If the donor energy $E_{\rm D} \leq \min E_{1s}(\mathbf{k}) = -574$ meV (e.g., $E_{\rm D} = -800$ meV), there are practically no electrons in the p-subbands, and the concentration n of charge carriers in the s-subband monotonically grows with the temperature (Fig. 4, curves *1–3* and *5–7*). At $E_{\rm D} < -574$ meV, every impurity concentration ($n_{\rm D} = 4.64 \times 10^{10}$ and 10^8 cm^{-2}) has a temperature interval, where the concentration n in the subbands changes weakly (curves *4* and *8*). The further temperature growth results in an increase of the charge carrier concentration in the superlattice. This behavior can be observed very pronouncedly for curve *4* ($E_{\rm D} = -500$ meV and $n_{\rm D} = 10^8$ cm^{-2}), which is characterized by a drastic increase of the concentration n at $T \geq 110$ K. The corresponding analysis testifies that this behavior of the function $n = n(T)$ is associated with electron transitions that arise at given temperatures from the valence band into the electron subbands of the superlattice.

From Fig. 4, one can also see that, at certain temperatures, the behavior of the function $n = n(T)$, provided a fixed donor concentration $n_{\rm D}$, does not depend on the energy of impurity ionization. In particular, at $n_{\rm D} = 10^8$ cm^{-2}, the values of dependences *1–4* become almost identical already at $T > 135$ K; at $n_{\rm D} = 4.64 \times 10^{10}$ cm^{-2}, dependences *5* ($E_{\rm D} = -800$ meV) and *6* ($E_{\rm D} = -650$ meV) become equal at $T > 285$ K.

The specific conductance of the superlattice depends on both the donor concentration and energy, as well as the temperature (Fig. 5). Taking the aforesaid into account, we obtain that the superlattice conductivity is mainly driven by the motion of electrons belonging to the 1s-subband in the electric field. Besides the electron concentration, the magnitude of specific conductance is also determined by the charge mobility.

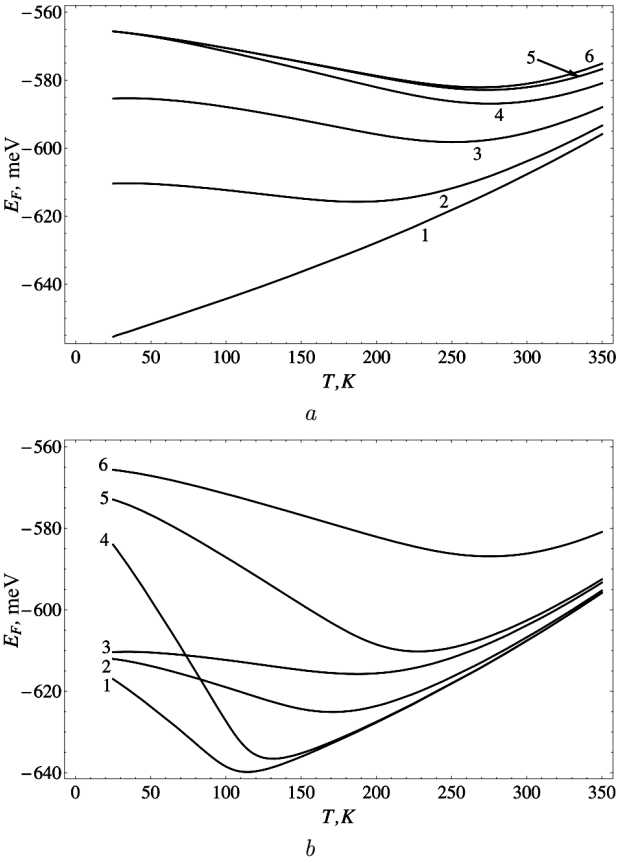

Fig. 3. Temperature dependences of the Fermi energy in the 2D superlattice InAs/GaAs with $R_{\rm NC} = 60$ Å. (*a*) $n_{\rm D} = 4.64 \times 10^{10}$ cm^{-2}; $E_{\rm D} = -850$ (*1*), -650 (*2*), -600 (*3*), -550 (*4*), -500 (*5*), and -300 meV (*6*). (*b*) $E_{\rm D} = -650$ meV corresponds to curves *1* to *3*, and $E_{\rm D} = -550$ meV to curves *4* to *6*; $n_{\rm D} = 10^8$ (*1, 4*), 10^{10} (*2, 5*), and 4.64×10^{10} cm^{-2} (*3, 6*)

From Fig. 5, one can see that all curves (*1–8*) in the temperature interval 130 K $< T <$ 170 K have a characteristic knee, which is associated with a drastic reduction of the relaxation time in this temperature interval. Like the carrier concentration case, we have two types of the T-dependence for the specific conductance at various energies $E_{\rm D}$. In particular, the function $\sigma = \sigma(T)$ decreases at $E_{\rm D} = -500$ meV (curves *4* and *8*) and monotonically increases at $E_{\rm D} < -500$ meV (curves *1–3* and *5–7*).

At temperatures close to room one ($T > 300$ K), the conductivity weakly depends on the impurity con-

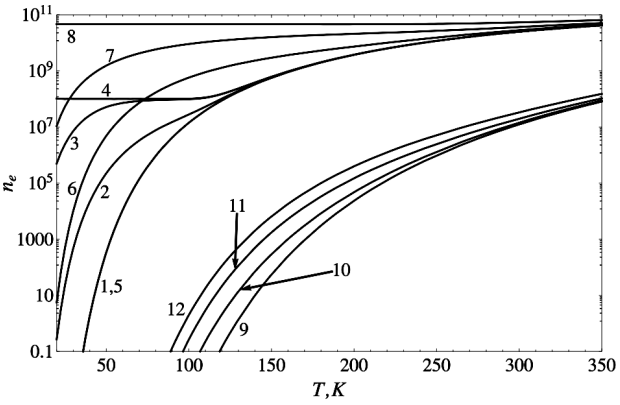

Fig. 4. Dependences of the charge carrier concentration in the 1*s*- and 1*p*-states on the temperature of InAs/GaAs 2D-superlattice with $R_{\rm NC} = 60$ Å: (*1–4*) 1*s*-subband, $n_{\rm D} = 10^8$ cm^{-2}; (*5–8*) 1s-subband, $n_{\rm D} = 4.64\times10^{10}$ cm^{-2}; (*9–12*) 1*p*-subband, $n_{\rm D} = 4.64 \times 10^{10}$ cm^{-2}; $E_{\rm D} = -800$ (*1, 5, 9*), -650 (*2, 6, 10*), -600 (*3, 7, 11*), and -500 meV (*4, 8, 12*)

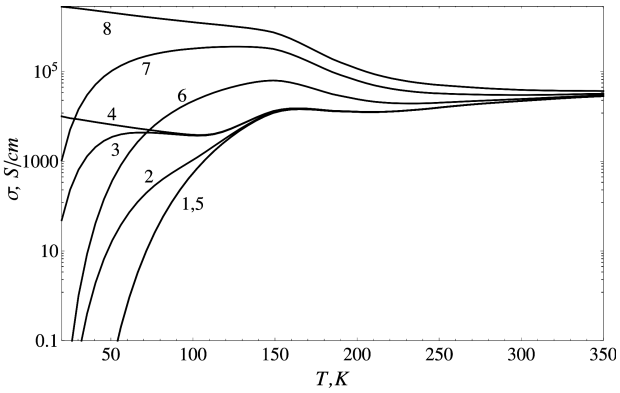

Fig. 5. Temperature dependences of the specific conductance of the 2D superlattice InAs/GaAs with $R_{\rm NC} = 60$ Å: $n_{\rm D} = 10^8$ (*1–4*) and 4.64×10^{10} cm^{-2} (*5–8*); $E_{\rm D} = -800$ (*1, 5*), -650 (*2, 6*), -600 (*3, 7*), and -500 meV (*4, 8*)

centration $n_{\rm D}$. This phenomenon can be explained by the fact that the role of electron transitions from the valence band into the electron subbands of the conduction band increases at those temperatures.

4. Conclusions

The electrical properties of superlattices of InAs quantum dots in the GaAs matrix have been analyzed. The superlattices with NC dimensions that allow the existence of several (1*s*- and 1*p*-like) electron subbarrier subbands are studied. The charge carriers in the subbands are assumed to be provided by thermally induced transitions from the levels of impurity atoms in the heterostructure and from the valence subbands (at high temperatures). Depending on the impurity level position with respect to the conduction band bottom in the semiconductor matrix, different temperature variations of the superlattice specific conductance and the impurity concentration are obtained. It is found that two types of the dependence $\sigma = \sigma(T)$ are possible, depending on the ratio between the impurity level energy and the energy at the boundary of the electron 1*s*-subband: in the interval of low and medium temperatures (up to room one), the conductivity can either decrease or increase as the temperature grows. The dependence $\sigma = \sigma(T)$ is obtained for the case of high temperatures, when the conductivity acquires the bipolar character (with the participation of both electrons and holes).

The proposed strong-coupling model is demonstrated to adequately describe the dispersion laws for electrons and holes in the subbarrier subbands, because our results agree with the data of works [26–31], where other models were used.

In this work, we assumed that InAs nanocrystals in the GaAs matrix have a spherical shape. Keeping in mind a definite restriction of this assumption, we would like to note that it is not always easy to experimentally determine a true shape of the nanocrystal surface in the matrix, when the nanocrystals are small ($a \leq 6$ nm). Moreover, as was shown in our works and the works of other authors, the NC volume is the most crucial parameter for the determination of the energy spectrum of charges in NCs, with the NC shape inserting only a correction to the energy value [12, 13, 35, 36]. The selected NC shape has an advantage, because we can use exact analytical expressions for the wave functions of electron and hole states in NCs.

The obtained results of calculations can be applied, when studying the photo-electrical properties of various heterosystems with periodically arranged nanocrystals.

1. I.D. Rukhlenko, D. Handapangoda, M. Premaratne, A.V. Fedorov, A.V. Baranov, C. Jagadish. Spontaneous emission of guided polaritons by quantum dot coupled to metallic nanowire: Beyond the dipole approximation. *Opt. Express* **17**, 17570 (2009) [DOI: 10.1364/OE.17.017570].

2. X.L. Wu, F.S. Xue. Optical transition in discrete levels of Si quantum dots. *Appl. Phys. Lett.* **84**, 2808 (2004) [DOI: /10.1063/1.1704872].
3. O.B. Shchekin, G. Park, D.L. Huffaker, D.G. Deppe. Discrete energy level separation and the threshold temperature dependence of quantum dot lasers. *Appl. Phys. Lett.* **77**, 466 (2000) [DOI: 10.1063/1.127012].
4. A.V. Fedorov, I.D. Rukhlenko, A.V. Baranov, S.Yu. Kruchinin. *Optical Properties of Semiconductor Quantum Dots* (Nauka, 2011) (in Russian).
5. *Semiconductor Quantum Dots,* edited by Y. Masumoto, T. Takagahara (Springer, 2002) [ISBN: 978-3-662-05001-9].
6. S.M. Reimann, M. Manninen. Electronic structure of quantum dots. *Rev. Mod. Phys.* **74**, 1283 (2002) [DOI: 10.1103/RevModPhys.74.1283].
7. A.D. Yoffe. Semiconductor quantum dots and related systems: Electronic, optical, luminescence and related properties of low dimensional systems. *Adv. Phys.* **50**, 1 (2001) [DOI: 10.1080/00018730010006608].
8. I.D. Rukhlenko, M.Y. Leonov, V.K. Turkov, A.P. Litvin, A.S. Baimuratov, A.V. Baranov, A.V. Fedorov. Kinetics of pulse-induced photoluminescence from a semiconductor quantum dot. *Opt. Express* **20**, 27612 (2012) [DOI: 10.1364/OE.20.027612].
9. A.S. Baimuratov. Shape-induced anisotropy of intraband luminescence from a semiconductor nanocrystal. *Opt. Lett.* **37**, 4645 (2012) [DOI: 10.1364/OL.37.004645].
10. D. Press, Th.D. Ladd, B. Zhang, Y. Yamamoto. Complete quantum control of a single quantum dot spin using ultrafast optical pulses. *Nature* **456**, 218 (2008) [DOI: 10.1038/nature07530].
11. A.V. Baranov, A.V. Fedorov, I.D. Rukhlenko, Y. Masumoto. Intraband carrier relaxation in quantum dots embedded in doped heterostructures. *Phys. Rev. B* **68**, 205318 (2003) [DOI: 10.1103/PhysRevB.68.205318].
12. V.I. Boichuk, I.V. Bilynskyi, R.Ya. Leshko, L.M. Turyanska. Optical properties of a spherical quantum dot with two ions of hydrogenic impurity. *Physica E* **54**, 281 (2013) [DOI: 10.1016/j.physe.2013.07.003].
13. V.I. Boichuk, I.V. Bilynsky, I.O. Shakleina, I. Kogoutiouk. Dielectric mismatch in finite barrier cubic quantum dots. *Physica E* **43**, 161 (2010) [DOI: 10.1016/j.physe.2010.06.031].
14. A.J. Shields. Semiconductor quantum light sources. *Nat. Photon.* **1**, 215 (2007) [DOI: 10.1038/nphoton.2007.46].
15. K.J. Vahala. Optical microcavities. *Nature* **424**, 839 (2003) [DOI: 10.1038/nature01939].
16. V.I. Klimov, A.A. Mikhailovsky, S. Xu, A. Malko. Optical gain and stimulated emission in nanocrystal quantum dots. *Science* **290**, 314 (2000) [DOI: 10.1126/science.290.5490.314].
17. Z.L. Yuan, B.E. Kardynal, R.M. Stevenson, A.J. Shields, C.J. Lobo, K. Cooper, N.S. Beattie, D.A. Ritchie, M. Pepper. Electrically driven single-photon source. *Science* **295**, 102 (2002) [DOI: 10.1126/science.1066790].
18. A.J. Bennett, D.C. Unitt, P. See, A.J. Shields, P. Atkinson, K. Cooper, D.A. Ritchie. Microcavity single-photon-emitting diode. *Appl. Phys. Lett.* **86**, 181102 (2005) [DOI: 10.1063/1.1921332].
19. P. Michler, A. Kiraz, C. Becher, W.V. Schoenfeld, P.M. Petroff, L. Zhang, E. Hu, A. Imamoglu. A quantum dot single-photon turnstile device. *Science* **290**, 2282 (2000) [DOI: 10.1126/science.290.5500.2282].
20. K. Tanabe, K. Watanabe, Y. Arakawa. III-V/Si hybrid photonic devices by direct fusion bonding. *Sci. Rep.* **2**, 349 (2012) [DOI: 10.1038/srep00349].
21. J. Jasieniak, B.I. MacDonald, S.E. Watkins, P. Mulvaney. Solution-processed sintered nanocrystal solar cells via layer-by-layer assembly. *Nano Lett.* **11**, 2856 (2011) [DOI: 10.1021/nl201282v].
22. I. Gur, N.A. Fromer, M.L. Geier, A.P. Alivisatos. Air-stable all-inorganic nanocrystal solar cells processed from solution. *Science* **310**, 462 (2005) [DOI: 10.1126/science.1117908].
23. P. Prabhakaran, W.J. Kim, K.S. Lee, P.N. Prasad. Quantum dots (QDs) for photonic applications. *Opt. Mater. Express* **2**, 578 (2012) [DOI: 10.1364/OME.2.000578].
24. S.A. McDonald, G. Konstantatos, S. Zhang, P.W. Cyr, E.J.D. Klem, L. Levina, E.H. Sargent. Solution-processed PbS quantum dot infrared photodetectors and photovoltaics. *Nat. Mater.* **4**, 138 (2005) [DOI: 10.1038/nmat1299].
25. D. Qi, M. Fischbein, M. Drndić, S. Šelmić. Efficient polymer-nanocrystal quantum-dot photodetectors. *Appl. Phys. Lett.* **86**, 093103 (2005) [DOI: 10.1063/1.1872216].
26. N.V. Tkach, A.M. Makhanets, G.G. Zegrya. Energy spectrum of electron in quasiplane superlattice of cylindrical quantum dots. *Semicond. Sci. Technol.* **15**, 395 (2000) [DOI: 10.1088/0268-1242/15/4/315].
27. N.V. Tkach, Yu.A. Seti. Optimization of the configuration of symmetric three-barrier resonance-tunnel structure as an active element of a quantum cascade detector. *Fiz. Tekh. Poluprovodn.* **45**, 387 (2011) (in Russian).
28. Ju.O. Seti, M.V. Tkach, I.V. Boyko. Influence of non-linear electrons interaction at their transport through the symmetric two- barrier resonance nano-system. *J. Optoelectron. Adv. Mater.* **14**, 393 (2012).
29. V.A. Holovatsky, V.I. Gutsul, O.M. Makhanets. Energy spectrum of electron in superlattice along the elliptic nanowire. *Rom. J. Phys.* **52**, 327 (2007).
30. O.L. Lazarenkova, A.A. Balandin. Miniband formation in a quantum dot crystal. *J. Appl. Phys.* **89**, 5509 (2001) [DOI: 10.1063/1.1366662].
31. O.L. Lazarenkova, A.A. Balandin. Electron and phonon energy spectra in a three-dimensional regimented quantum dot superlattice. *Phys. Rev. B* **66**, 245319 (2002) [DOI: 10.1103/PhysRevB.66.245319].
32. V.I. Boichuk, I.V. Bilynsky, R.I. Pazyuk, I.O. Shakleina. Energy spectrum of charges in a periodic system of spherical quantum dots. *Fiz. Khim. Tverd. Tila* **10**, 752 (2009) (in Ukrainian).

33. V.I. Boichuk, I.V. Bilynsky, R.I. Pazyuk. Coefficient of light absorption induced by electron intersubband transitions in superlattices of spherical quantum dots. *Zh. Fiz. Dosl.* **19**, 1601 (2015) (in Ukrainian).
34. V. Boichuk. *Fundamentals of Solid State Theory: A Tutorial* (Kolo, 2010) (in Ukrainian).
35. R. Mohan, Y. Liang. Intersublevel relaxation properties of self-assembled InAs/GaAs quantum dot heterostructures. In *Cutting Edge Nanotechnology* (InTech, 2010), p. 316 [ISBN: 978-953-7619-93-0].
36. V.I. Boichuk, I.V. Bilynskyi, O.A. Sokolnyk, I.O. Shakleina. Effect of quantum dot shape of the GaAs/AlAs heterostructure on interlevel hole light absorption. *Cond. Matter Phys.* **16**, 33702 (2013) [DOI: 10.5488/CMP.16.33702].

Received 04.07.16
Translated from Ukrainian by O.I. Voitenko

В.І. Бойчук, І.В. Білинський, Р.І. Пазюк

МІНІЗОННА ЕЛЕКТРОПРОВІДНІСТЬ
У НАДҐРАТКАХ СФЕРИЧНИХ КВАНТОВИХ
ТОЧОК ГЕТЕРОСИСТЕМИ InAs/GaAs

Р е з ю м е

В роботі досліджуються електричні властивості напівпровідникових наногетеросистем InAs/GaAs з 2D-надґратками сферичних квантових точок. Отримані залежності групової швидкості електронів від хвильового вектора та номера мінізони. Встановлено залежність рівня Фермі системи електронів в мінізонах від концентрації донорних домішок, енергії їх залягання та температури. Досліджено температурну залежність концентрації основних носіїв та електропровідності для різних значень концентрації та енергії залягання донорів.